4212 *Inorg. Chem.* **2010**, *49*, 4212–4223
DOI: 10.1021/ic902461g

Inorganic Chemistry
Article

Molecular Recognition of Sialic Acid by Lanthanide(III) Complexes through Cooperative Two-Site Binding

Martín Regueiro-Figueroa,[†] Kristina Djanashvili,[‡] David Esteban-Gómez,[†] Thomas Chauvin,[§] Éva Tóth,[§] Andrés de Blas,[†] Teresa Rodríguez-Blas,*[,†] and Carlos Platas-Iglesias*[,†]

[†]*Departamento de Química Fundamental, Universidade da Coruña, Campus da Zapateira, Alejandro de la Sota 1, 15008 A Coruña, Spain,* [‡]*Biocatalysis and Organic Chemistry, Department of Biotechnology, Delft University of Technology, Julianalaan 136, 2628 BL Delft, The Netherlands, and* [§]*Centre de Biophysique Moléculaire, CNRS, rue Charles Sadron, 45071 Orléans Cedex 2, France*

Received December 11, 2009

Herein we report two new ligands, 1,4,7-tris(carboxymethyl)-10-[2-(dihydroxyboranyl)benzyl]-1,4,7,10-tetraazacyclododecane (L^1) and 1,4,7-tris(carboxymethyl)-10-[3-(dihydroxyboranyl)benzyl]-1,4,7,10-tetraazacyclododecane (L^2), which contain a phenylboronic acid (PBA) function and a 1,4,7,10-tetraazacyclododecane-1,4,7-triacetate cage for complexation of lanthanide ions in an aqueous solution. The pK_a of the PBA function amounts to 4.6 in [Gd(L^1)] and 8.9 in [Gd(L^2)], with the value of the L^2 analogue being very similar to that of PBA (8.8). These results are explained by the coordination of the PBA function of L^1 to the Gd^{III} ion, which results in a dramatic lowering of its pK_a. As a consequence, [Gd(L^1)] does not bind to saccharides at physiological pH. The nuclear magnetic relaxation dispersion profiles recorded for [Gd(L^1)] and [Gd(L^2)] confirm that the phenylboronate function is coordinated to the metal ion in the L^1 derivative, which results in a q=0 complex. The interaction of the [Gd(L^2)] complex with 5-acetylneuraminic acid (Neu5Ac) and 2-α-*O*-methyl-5-acetylneuraminic acid (MeNeu5Ac) has been investigated by means of spectrophotometric titrations in an aqueous solution (pH 7.4, 0.1 M 3-(*N*-morpholino)propanesulfonic acid buffer). Furthermore, we have also investigated the binding of these receptors with competing monosaccharides such as D-(+)-glucose, D-fructose, D-mannose, D-galactose, methyl α-D-galactoside, and methyl α-D-mannoside. The binding constants obtained indicate an important selectivity of [Gd(L^2)] for Neu5Ac (K_{eq} = 151) over D-(+)-glucose (K_{eq} = 12.3), D-mannose (K_{eq}=21.9), and D-galactose (K_{eq}=24.5). Furthermore, a very weak binding affinity was observed in the case of methyl α-D-galactoside and methyl α-D-mannoside. An 8-fold increase of the binding constant of [Gd(L^2)] with Neu5Ac is observed when compared to that of PBA determined under the same conditions (K_{eq} = 19). ^{13}C NMR spectroscopy and density functional theory calculations performed at the B3LYP/6-31G(d) level show that this is due to a cooperative two-site binding of Neu5Ac through (1) ester formation by interaction on the PBA function of the receptor and (2) coordination of the carboxylate group of Neu5Ac to the Gd^{III} ion. The emission lifetime of the $^5D_4$ level of Tb^{III} in [Tb(L^2)] increases upon Neu5Ac binding, in line with the displacement of inner-sphere water molecules due to coordination of Neu5Ac to the metal ion.

Introduction

Lanthanide chelates with macrocyclic ligands are of great interest because they are used both as contrast agents for magnetic resonance imaging[1] and as radiopharmaceuticals for the diagnosis and therapy of tumors.[2] An important goal of the research in this field is to achieve a precise delivery of these compounds to specific targets in vivo.[3] The general strategy used for this purpose is to attach to these chelates bioconjugates or recognition moieties that could bind to specific receptors that are overexpressed in certain tissues. For instance, sialic acid is considered to be a tumor marker because it is known to be overexpressed on the surface of tumor cells.[4] Variations in the amount of sialic acid incorporated have been correlated with colon cancer, brain tumors, and immune regulation in the human body.[5] Moreover, serum levels of sialic acid can be used as a biological marker

*To whom correspondence should be addressed. E-mail: cplatas@udc.es (C.P.-I.), mayter@udc.es (T.R-B.).

(1) *The Chemistry of Contrast Agents in Medical Magnetic Resonance Imaging*; Merbach, A. E., Tóth, É., Eds.; Wiley: New York, 2001.

(2) (a) Liu, S. *Adv. Drug Delivery Rev.* **2008**, *60*, 1347–1370. (b) Roesch, F. *Radiochim. Acta* **2007**, *95*, 303–311. (c) Volkert, W. A.; Hoffman, T. J. *Chem. Rev.* **1999**, *99*, 2269–2292. (d) De Jong, M.; Breeman, W. A. P.; Kwekkeboom, E. J.; Valkema, R.; Krenning, E. P. *Acc. Chem. Res.* **2009**, *42*, 873–880.

(3) (a) De Leon-Rodriguez, L. M.; Lubag, A. J. M.; Malloy, C. R.; Martinez, G. V.; Gillies, R. J.; Sherry, A. D. *Acc. Chem. Res.* **2009**, *42*, 948–957. (b) Caravan, P. *Acc. Chem. Res.* **2009**, *42*, 851–862. (c) De Leon-Rodriguez, L. M.; Kovacs, Z. *Bioconjugate Chem.* **2008**, *19*, 391–402. (d) Aime, S.; Crich, S. G.; Gianolio, E.; Giovenzana, G. B.; Tei, L.; Terreno, E. *Coord. Chem. Rev.* **2006**, *250*, 1562–1579.

(4) Schauer, R. *Glycoconjugate J.* **2000**, *17*, 485–499.

(5) Dall'Olio, F.; Chiricolo, M. *Glycoconjugate J.* **2001**, *18*, 841–850.

 Published on Web 04/07/2010

Chart 1. 5-Acetylneuraminic Acid (**1**, Neu5Ac) and 2-α-*O*-Methyl-5-acetylneuraminic Acid (**2**, MeNeu5Ac)

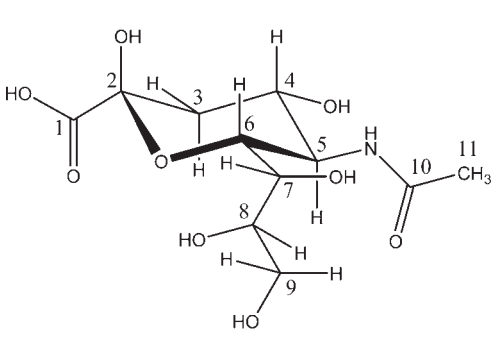

1

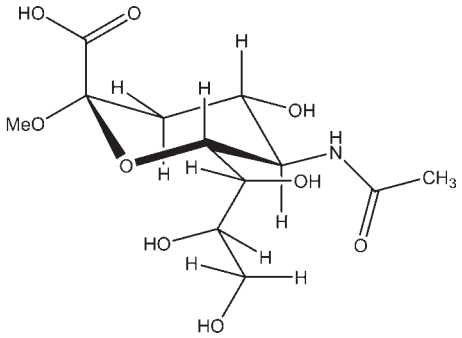

2

of a cancerous state.[6] Thus, molecular recognition of sialic acid is important to developing assays that could enable the enhanced detection of malignancies and other diseases involving high sialic acid levels. Sialic acids contain the nine-carbon amino sugar neuraminic acid, with the most common member of this family being 5-acetylneuraminic acid (Neu5Ac; Chart 1).[7] Sialic acids contain a carboxy group at the anomeric carbon atom that gives the molecule a negative charge at physiological pH. Neu5Ac and its derivatives generally occupy the terminal positions of carbohydrate chains of glycoproteins and glycolipids in biological membranes, and they appear to play important roles in cellular recognition processes.[8] Neu5Ac is present in an aqueous solution as an equilibrium between α-pyranose (5−8%) and *β*-pyranose forms (92−95%), while the furanose type of Neu5Ac is absent because of the acetamide moiety present at the C5 position.[9] In addition to these cyclic forms, three acyclic forms have been recently detected at low levels (0.5−1.9% at pH 2).[10] However, it must be pointed out that all known glycosides of Neu5Ac are α-linked, often to a galactose or a *N*-galactosamine residue through a α(2→3) or α(2→6) linkage.[11]

Boronic acids are a promising class of recognition moieties for the synthesis of artificial receptors and sensors for α-hydroxycarboxylates[12] or molecules containing diol groups[13] such as saccharides.[14] The use of boronic acids for this purpose is based on their ability to form reversible covalent complexes with 1,2- and 1,3-diol units in saccharides.[15] Detailed investigations on the interaction of Neu5Ac with phenylboronic acid (PBA)[16] and PBA derivatives[17] have been reported in the literature. A noninvasive method for the detection of sialic acid at the cell membrane by using a PBA monolayer gold electrode has also been reported recently.[18] It has been suggested that more selective artificial receptors for sialic acid residues in glycoproteins or free sialic acid should contain both a PBA function and a group capable of recognizing the negatively charged COO^- group of sialic acid (Chart 1). This has been achieved by the introduction of positively charged units, such as ammonium groups, in the framework of the receptor.[19−21] A second strategy uses diboronate receptors, which can bind free sialic acid through both the glycerol side chain and the α-hydroxy acid function at the anomeric position (Chart 1).[22] A third approach consists of the use of a metal chelate, typically a Zn^{II} or Cu^{II} complex, to promote a cooperative binding of boronic acid and metal chelate. Indeed, Shinkai et al. have developed a fluorescent sensor containing a PBA moiety that is able to interact with diols and a positively charged 1,10-phenanthrolinezinc(II) chelate moiety for carboxylate binding.[23]

A few conjugates of PBA and lanthanide(III) complexes of diethylenetriaminepentaacetate (DTPA),[20,24] diethylenetriaminepentaacetate bisamides,[21] and 1,4,7,10-tetraazacyclododecane-1,4,7,10-tetraacetate (DOTA) tetraamides[25] have been reported in the literature. These conjugates contain

(6) Krolikowski, F. J.; Reuter, K.; Waalkes, T. P.; Sieber, S. M.; Adamson, R. H. *Pharmacology* **1976**, *14*, 47–51.
(7) Schauer, R. *Zoology* **2004**, *107*, 49–64.
(8) Varki, A. *Trends Mol. Med.* **2008**, *14*, 351–360.
(9) Friebolin, H.; Kunzelmann, P.; Supp, M.; Brossmer, R.; Keilich, G.; Ziegler, D. *Tetrahedron Lett.* **1981**, *22*, 1383–1386.
(10) Klepach, T.; Carmichael, I.; Serianni, A. S. *J. Am. Chem. Soc.* **2008**, *130*, 11892–11900.
(11) (a) Varki, A. *Nature* **2007**, *446*, 1023–1029. (b) Murrey, H. E.; Hsieh-Wilson, C. *Chem. Rev.* **2008**, *108*, 1708–1731. (c) Angata, T.; Varki, A. *Chem. Rev.* **2002**, *102*, 439–469.
(12) (a) Zhu, L.; Zhong, Z.; Anslyn, E. V. *J. Am. Chem. Soc.* **2005**, *127*, 4260–4269. (b) Zhang, X.; Chi, L.; Ji, S.; Wu, Y.; Song, P.; Han, K.; Guo, H.; James, T. D.; Zhao, J. *J. Am. Chem. Soc.* **2009**, *131*, 17452–17463.
(13) Shabbir, S. H.; Joyce, L. A.; da Cruz, G. M.; Lynch, V. M.; Sorey, S.; Anslyn, E. V. *J. Am. Chem. Soc.* **2009**, *131*, 13125–13131.
(14) (a) Mader, H. S.; Wolfbeis, O. S. *Microchim. Acta* **2008**, *162*, 1–34. (b) James, T. D. *Top. Curr. Chem.* **2007**, *277*, 107–152. (c) James, T. D.; Shinkai, S. *Top. Curr. Chem.* **2002**, *218*, 159–200. (d) James, T. D.; Tony, D.; Sandanayake Samankumara, K. R. A.; Shinkai, S. *Angew. Chem., Int. Ed.* **1996**, *35*, 1911–1922. (e) Zhang, T.; Anslyn, E. V. *Org. Lett.* **2007**, *9*, 1627–1629.
(15) Fujita, N.; Shinkai, S.; James, T. D. *Chem. Asian J.* **2008**, *3*, 1076–1091.
(16) Djanashvili, K.; Frullano, L.; Peters, J. A. *Chem.—Eur. J.* **2005**, *11*, 4010–4018.
(17) Otsuka, H.; Uchimura, E.; Koshino, H.; Okano, T.; Kataoka, K. *J. Am. Chem. Soc.* **2003**, *125*, 3493–3502.
(18) Matsumoto, A.; Sato, N.; Kataoka, K.; Miyahara, Y. *J. Am. Chem. Soc.* **2009**, *131*, 12022–12023.
(19) Patterson, S.; Smith, B. D.; Taylor, R. A. *Tetrahedron Lett.* **1998**, *39*, 3111–3114.
(20) Battistini, E.; Mortillaro, A.; Aime, S.; Peters, J. A. *Contrast Media Mol. Imaging* **2007**, *2*, 163–171.
(21) (a) Frullano, L.; Rohovec, J.; Aime, S.; Maschmeyer, T.; Prata, M. I.; Pedroso de Lima, J. J.; Geraldes, C. F. G. C.; Peters, J. A. *Chem.—Eur. J.* **2004**, *10*, 5205–5217. (b) Djanashvili, K.; Koning, G. A.; van der Meer, A. J. G. M.; Wolterbeek, H. T.; Peters, J. A. *Contrast Media Mol. Imaging* **2007**, *2*, 35–41.
(22) Levonis, S. M.; Kiefel, M. J.; Houston, T. A. *Chem. Commun.* **2009**, 2278–2280.
(23) (a) Yamamoto, M.; Takeuchi, M.; Shinkai, S. *Tetrahedron* **1998**, *54*, 3125–3140. (b) Takeuchi, M.; Yamamoto, M.; Shinkai, S. *Chem. Commun.* **1997**, 1731–1732.
(24) Takahashi, K.; Nakamura, H.; Furumoto, S.; Yamamoto, K.; Fukuda, H.; Matsumura, A.; Yamamoto, Y. *Bioorg. Mol. Chem.* **2005**, *13*, 735–743.
(25) (a) Trokowski, R.; Zhang, S.; Sherry, A. D. *Bioconjugate Chem.* **2004**, *15*, 1431–1440. (b) Zhang, S.; Trokowski, R.; Sherry, A. D. *J. Am. Chem. Soc.* **2003**, *125*, 15288–15289. (c) Ren, J.; Trokowski, R.; Zhang, S.; Malloy, C. R.; Sherry, A. D. *Magn. Reson. Med.* **2008**, *60*, 1047–1055.

Chart 2. Ligands Reported in This Work

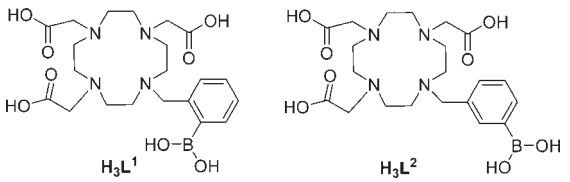

octadentate binding units for coordination of the Ln^{III} ions, which therefore are not expected to participate in molecular recognition processes. Lanthanide(III) complexes with heptadentate ligands such as 1,4,7,10-tetraazacyclododecane-1,4,7-triacetate (DO3A) derivatives are typically diaqua systems that are known to bind different oxyanions, which replace inner-sphere water molecules to give $q = 0$ complexes.[26] A suitable receptor for sialic acid recognition could therefore be based on a Ln(DO3A) complex, which could bind the carboxylate function of sialic acid, attached to a PBA function for recognition of the 1,2- and 1,3-diol groups of Neu5Ac. Thus, herein we report receptors H_3L^1 and H_3L^2, which contain a PBA function attached to a nitrogen atom of a DO3A backbone (Chart 2). The presence of these two recognition units is expected to increase the specificity and stability of the interaction between the corresponding lanthanide complexes and sialic acid. Furthermore, the lanthanide(III) complexes of these ligands were designed to interact reversibly with sialic acid. Interaction of the lanthanide(III) complexes of L^1 and L^2 with Neu5Ac and other competing monosaccharides was investigated in aqueous solutions by means of spectrophotometric titrations and ^1H, ^{13}C, and ^{11}B NMR spectroscopies, as well as by density functional theory (DFT) calculations performed at the B3LYP/6-31G(d) level. The potential interference of α-hydroxy acid species present in vivo, such as lactate and citrate, was also analyzed. Furthermore, we also investigated the interaction of these complexes with 2-α-*O*-methyl-5-acetylneuraminic acid (MeNeu5Ac) as a model for cell-bound neuraminic residues, which are α-linked via the −OH group in position 2.[9] Finally, the nuclear magnetic relaxation dispersion (NMRD) profiles of the gadolinium(III) complexes are reported.

Results and Discussion

Synthesis of the Ligands. The synthetic strategy used for the preparation of H_3L^1 is outlined in Scheme 1. In a first attempt toward L^1, we decided to prepare the 2-(bromomethyl)phenyl borate ester **4**.[27] The latter compound was obtained in two steps from commercially available *o*-tolylboronic acid, which was reacted with 2,2-dimethyl-1,3-propanediol to give the protected 2-phenylboronic acid **3**. Free-radical bromination of **3** with *N*-bromosuccinimide (NBS) and dibenzoyl peroxide (PDB) afforded compound **4**

Scheme 1. Synthesis of Ligand H_3L^1

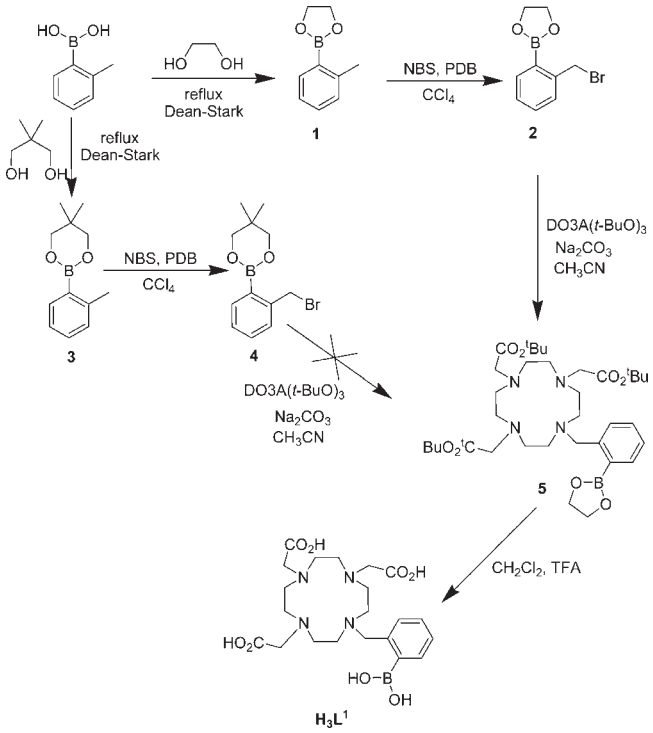

in 82% yield. However, N-alkylation reactions[28] of 1,4,7-tris[(*tert*-butoxycarbonyl)methyl]-1,4,7,10-tetraazacyclododecane [DO3A(*t*-BuO)$_3$] with **4** in refluxing acetonitrile in the presence of Na_2CO_3 did not provide any results. Most likely, the presence of the bulky protecting group in **4** causes some steric hindrance that prevents the N-alkylation. As an alternative, we decided to prepare [2-(bromomethyl)phenyl]ethylene borate (**2**).[29] The treatment of DO3A(*t*-BuO)$_3$ with **2** in refluxing acetonitrile in the presence of Na_2CO_3, followed by purification with column chromatography, afforded the pure protected precursor **5** in 63% yield. Finally, full deprotection of the *tert*-butyl esters and PBA function was achieved with trifluoroacetic acid (TFA), providing the desired ligand as the trifluoroacetate salt in 75% yield. The synthesis of $H_3L^2 \cdot 3CF_3COOH$ was achieved from *m*-tolylboronic acid following an analogous synthetic procedure.

Synthesis and Characterization of the Complexes. Ligands H_3L^1 and H_3L^2 were derivatized to form several charge-neutral lanthanide complexes of formulas $[Ln(L^1)] \cdot 2H_2O$ and $[Ln(L^2)] \cdot 4H_2O$ (Ln = La, Eu, Gd, or Tb), which were obtained in 54−79% yield by reaction of the ligand with equimolar amounts of the corresponding lanthanide triflate in the presence of triethylamine. The mass spectra of the complexes (positive ion electrospray ionization, ESI^+) show intense peaks due to $[Ln(HL^1)]^+$ and $[Ln(HL^2)]^+$ entities, which confirms the formation of the desired complexes.

The pK_a values of PBAs can be determined following the change in the UV absorption that occurs when the boron atom converts from the tetrahedral to the trigonal

(26) (a) Dickins, R. S.; Aime, S.; Batsanov, A. S.; Beeby, A.; Botta, M.; Bruce, J. I.; Howard, J. A. K.; Love, C. S.; Parker, D.; Peacock, R. D.; Puschmann, H. *J. Am. Chem. Soc.* **2002**, *124*, 12697–12705. (b) Aime, S.; Botta, M.; Bruce, J. I.; Mainero, V.; Parker, D.; Terreno, E. *Chem. Commun.* **2001**, 115–116. (c) Bruce, J. I.; Dickins, R. S.; Govenlock, L. J.; Gunnlaugsson, T.; Lopinski, S.; Lowe, M. P.; Parker, D.; Peacock, R. D.; Perry, J. J. B.; Aime, S.; Botta, M. *J. Am. Chem. Soc.* **2000**, *122*, 9674–9684. (d) Terreno, E.; Botta, M.; Boniforte, P.; Bracco, C.; Milone, L.; Mondito, B.; Uggeri, F.; Aime, S. *Chem.—Eur. J.* **2005**, *11*, 5531–5537.

(27) (a) James, T. D.; Sandanayake, K. R. A. S.; Iguchi, R.; Shinkai, S. *J. Am. Chem. Soc.* **1995**, *117*, 8982–8987. (b) Stones, D.; Manku, S.; Lu, X.; Hall, D. G. *Chem.—Eur. J.* **2004**, *10*, 92–100.

(28) Barge, A.; Tei, L.; Upadhyaya, D.; Fedeli, F.; Beltrami, L.; Stefania, R.; Aime, S.; Cravotto, G. *Org. Biomol. Chem.* **2008**, *6*, 1176–1184.

(29) Glennon, J. D.; Walker, A.; Mckervey, M. A. *ARKIVOC* **2003**, *7*, 402–411.

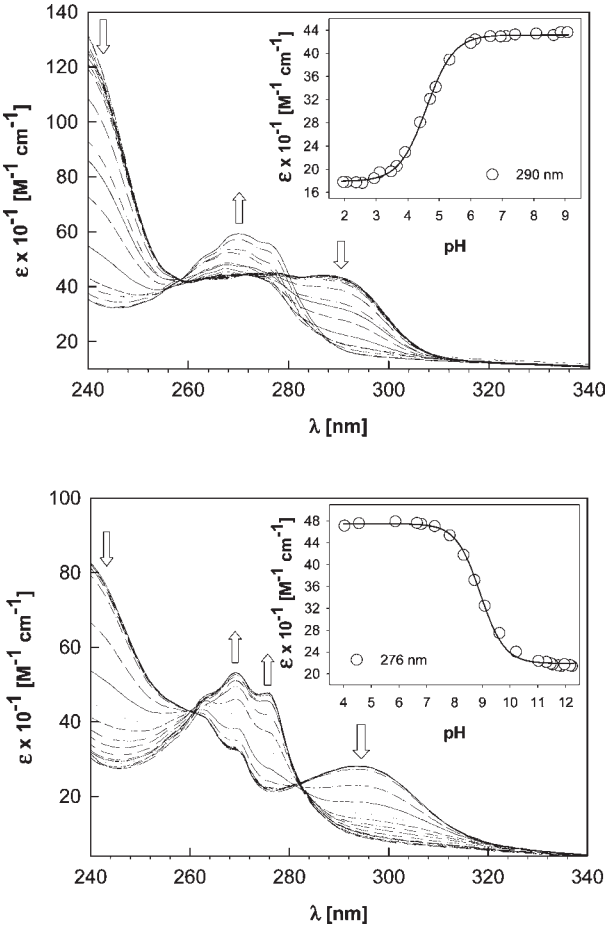

Figure 1. Spectrophotometric titrations of a 10^{-3} M aqueous solution of [Gd(L^1)] (top) and [Gd(L^2)] (bottom) with a standard HCl solution. Insets: changes in the molar absorbance at selected wavelengths as a function of the pH. The solid lines represent the best fittings of the experimental data.

planar form.[30] The UV−vis absorption spectra of the [Gd(L^1)] and [Gd(L^2)] complexes recorded at pH 12.0 [I = 0.1 M KCl] show a maximum at ∼290 nm. Upon a decrease in the pH of the solution, the intensity of this band decreases, while the formation of a new band with a maximum at 270 nm is observed (Figure 1). This band can be assigned as a $\pi^* \leftarrow \pi$ singlet−singlet transition centered on the trigonal-planar PBA unit (^1L_b transition according to the suggestion of Ramsey).[31] Analysis of the titration profiles provides very different pK_a values for the two complexes: 4.6 and 8.9 for the complexes of L^1 and L^2, respectively. The pK_a determined for [Gd(L^2)] is very similar to that determined by the same method for PBA itself (pK_a = 9.0; Figure S1 in the Supporting Information) as well as to that reported previously for PBA (pK_a = 8.8).[32] These results can be only explained by coordination of the PBA function of L^1 to the Gd^{III} ion, which results in a dramatic lowering of its pK_a. The ^{11}B NMR spectrum of a 10 mM aqueous solution of [La(L^2)] recorded at pH 1.6 shows a single resonance at 10 ppm. Increasing the pH of the solution provokes an upfield shift of the ^{11}B NMR signal to ca. −20 ppm due to conversion of the boronic acid function from the tetrahedral to the trigonal planar form (Figure S2 in the Supporting Information). Analysis of the ^{11}B NMR titration profile provides a pK_a of 8.9, in nice agreement with the value obtained from spectrophotometric titrations.

Table 1. Luminescence Emission Lifetimes of [Tb(L^1)] and [Tb(L^2)] in H_2O and D_2O Solutions at 25 °C and pH 7.4 (0.1 M MOPS Buffer) and Calculated Hydration Numbers (q)[a]

	$\tau(H_2O)$/ms	$\tau(D_2O)$/ms	q^a	q^b
[Tb(L^1)]	1.69	2.05	0.4	0.2
[Tb(L^2)]	1.18	1.88	1.3	1.3

[a] Equation 1. [b] Equation 2.

Luminescence lifetime measurements have been widely used for quantification of the number of inner-sphere water molecules in lanthanide complexes.[33] Although ions that emit in the near-infrared such as Yb^{III} have also been used for this purpose, Tb^{III} and Eu^{III} are most commonly applied for lifetime measurements because they emit in the visible region and show longer emission lifetimes. Unfortunately, the europium(III) complexes of L^1 and L^2 do not show Eu^{III}-centered emission upon excitation through the PBA chromophore at 270 nm. However, the emission spectrum of the terbium(III) analogues recorded at pH 7.4 [0.1 M 3-(*N*-morpholino)propanesulfonic acid (MOPS)] shows the typical $^5D_4 \rightarrow {}^7F_J$ transitions with maxima at ca. 621 (J = 3), 587 (J = 4), 545 (J = 5), and 490 nm (J = 6) (Figure S3 in the Supporting Information). The emission lifetimes of the Tb($^5D_4$) excited-state levels have been measured in D_2O and H_2O solutions of the complexes (Table 1) and were used to calculate the number of coordinated water molecules q according to eqs 1,[34] and 2:[35]

$$q = 4.2\Delta k_{obs} \quad (1)$$

$$q = 5.0(\Delta k_{obs} - 0.06) \quad (2)$$

where $\Delta k_{obs} = k_{obs}(H_2O) - k_{obs}(D_2O)$ and $k_{obs} = 1/\tau_{obs}$. For [Tb(L^2)], we obtain q = 1.3, which suggests the presence of an equilibrium in an aqueous solution involving q = 2 and 1 complex species. Average hydration numbers of 1.3−1.4 have been previously obtained for different terbium(III) complexes with DO3A-like binding sites.[36] For [Tb(L^1)], we obtain clearly longer emission lifetimes than those for the L^2 analogue, in line with the replacement of inner-sphere water molecules by coordination of the PBA function to the metal ion. The q values obtained suggest that only one OH oscillator is coordinating to the lanthanide ion, which can be accounted for by coordination of a −OH group of the PBA function. These results suggest that in the terbium(III) complex of

(30) Soundararajan, S.; Badawi, M.; Kohlrust, C. M.; Hageman, J. H. *Anal. Biochem.* **1989**, *178*, 125–134.
(31) Ramsey, B. G. *J. Phys. Chem.* **1970**, *74*, 2464–2469.
(32) Yan, J.; Springsteen, G.; Deeter, S.; Wang, B. *Tetrahedron* **2004**, *60*, 11205–11209.
(33) Horrocks, W. D., Jr.; Sudnick, D. R. *Acc. Chem. Res.* **1981**, *14*, 384–392.
(34) Horrocks, W. D., Jr.; Sudnick, D. R. *J. Am. Chem. Soc.* **1979**, *101*, 334–340.
(35) Beeby, A.; Clarkson, I. M.; Dickins, R. S.; Faulkner, S.; Parker, D.; Royle, L.; de Sousa, A. S.; Williams, J. A. G.; Woods, M. *J. Chem. Soc., Perkin Trans. 2* **1999**, 493–504.
(36) Faulkner, S.; Pope, S. J. A. *J. Am. Chem. Soc.* **2003**, *125*, 10526–10527.

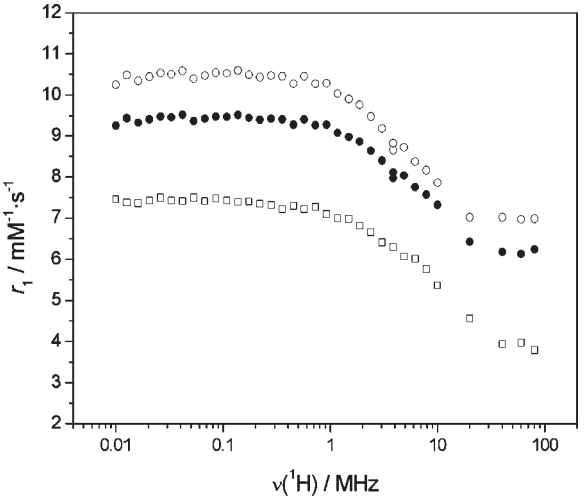

Figure 2. ^{1}H NMRD profiles (25 °C) of [Gd(L^1)] (□, 0.979 mM), [Gd(L^2)] (○, 1.62 mM), and [Gd(L^2)] (●, 1.62 mM) upon the addition of 10 equiv of Neu5Ac.

L^1 coordination of the PBA function does not allow coordination of water molecules to the metal ion, resulting in a $q = 0$ complex.

NMRD profiles of [Gd(L^1)] and [Gd(L^2)] (Figure 2; see also Figure S4 in the Supporting Information) were recorded at 25 and 37 °C (pH 7.4, *N*-2-(hydroxyethyl)-piperazine-*N*'-2-ethanesulfonic acid buffer). The relaxation rates of the bulk water protons are enhanced around a paramagnetic ion because of long-range interactions (outer-sphere relaxation) and short-range interactions (inner-sphere relaxation). According to the standard Solomon−Bloembergen−Morgan model, the latter process is governed by four correlation times: the rotational correlation time of the complex (τ_R), the residence time of a water proton in the inner coordination sphere (τ_m), and the longitudinal and transverse electronic relaxation times (T_{1e} and T_{2e}) of the metal center.[37] The shape of the NMRD profiles recorded for [Gd(L^1)] and [Gd(L^2)] (Figure 2) is similar to those of other low-molecular-weight DOTA-type chelates of gadolinium(III). The relaxivity values obtained for [Gd(L^1)] are clearly lower than those obtained for the L^2 analogue, in line with a lower hydration number of the former because of coordination of the phenylboronate pendant arm. The NMRD profile of [Gd(L^2)] recorded at 25 °C is very similar to that reported for [Gd(DO3A)],[38] which suggests that both complexes present similar hydration numbers. In the case of [Eu(DO3A)], a hydration equilibrium between $q = 2$ and 1 complex species with an average hydration number of $q = 1.88$ was established on the basis of UV−vis measurements.[39] The relaxivity values therefore suggest that for [Gd(L^2)] the hydration equilibrium is shifted to the $q = 2$ species and that our luminescence measurements on the terbium(III) complex underestimate the number of inner-sphere water molecules. This is in line with previous investigations that showed that luminescence emission lifetime measurements on terbium(III) complexes sometimes give lower q values than data collected on the corresponding europium(III) complex, in full accordance with the lanthanide contraction.[40]

Aiming to obtain information on the solution structure of the lanthanide(III) complexes of L^1 and L^2, we have performed DFT calculations at the B3LYP level. On the grounds of our previous experience,[41] in these calculations, we used the effective core potential (ECP) of Dolg et al.[42] and the related [5s4p3d]-GTO valence basis set for gadolinium, while the remaining atoms were described by using the 6-31G(d) basis set. Luminescence lifetime measurements performed on the terbium(III) complex of L^1 indicate that the PBA function is involved in coordination to the lanthanide, which results in a $q = 0$ complex. Furthermore, the boron atom of the ligand is expected to be in the tetrahedral form at neutral pH (see above). However, in the case of L^2 complexes, both luminescence emission lifetimes and relaxivity measurements point to an equilibrium involving $q = 1$ and 2 complexes, with the boron atom of the ligand being in the trigonal planar form at neutral pH. Thus, we performed our calculations on the [Gd(L^1OH)]$^-$, [Gd(L^2)(H_2O)], and [Gd(L^2)(H_2O)$_2$] systems.

It is well-known that in Ln^{III}(DOTA)-like complexes the four ethylenediamine groups adopt gauche conformations, giving rise to two macrocyclic ring conformations: ($\delta\delta\delta\delta$) and ($\lambda\lambda\lambda\lambda$). Furthermore, there are two possible orientations of the pendant arms (absolute configuration Δ or Λ), resulting in four possible steroisomers, existing as two enantiomeric pairs. These stereoisomers differ by the layout of the four acetate arms, adopting either a square-antiprismatic (SAP) or a twisted square-antiprismatic (TSAP) geometry.[43] The two structures display a different orientation of the two square planes formed by the four cyclen nitrogen atoms and the four binding oxygen atoms, making an angle of ca. 40° in SAP-type structures, whereas this situation is reversed and reduced to ca. −30° in TSAP-type derivatives.[44] As expected, our calculations performed in the gas phase provide the SAP [Δ($\lambda\lambda\lambda\lambda$)] and TSAP [Δ($\delta\delta\delta\delta$)] isomers as minimum-energy conformations for all complexes. Furthermore, the PBA function of L^1 can coordinate to the Gd^{III} ion by adopting syn or anti conformations.[45] In the syn isomer, the orientation of the PBA function follows the direction of rotation of the acetate arms, while in the anti

(37) Peters, J. A.; Huskens, J.; Raber, D. J. *Prog. Magn. Reson. Spectrosc.* **1996**, *28*, 283–350.
(38) Aime, S.; Botta, M.; Geninatti Crich, S.; Giovenzana, G.; Pagliarin, R.; Sist., M.; Terreno, E. *Magn. Reson. Chem.* **1998**, *36*, S200–S208.
(39) Toth, E.; Ni Dhubhghaill, O. M.; Besson, G.; Helm, L.; Merbach, A. E. *Magn. Reson. Chem.* **1999**, *37*, 701–708.
(40) Woods, M.; Aime, S.; Botta, M.; Howard, J. A. K.; Molones, J. M.; Navet, M.; Parker, D.; Port, M.; Rousseaux, O. *J. Am. Chem. Soc.* **2000**, *122*, 9781–9792.
(41) (a) Roca Sabio, A.; Mato-Iglesias, M.; Esteban-Gomez, D.; Toth, E.; de Blas, A.; Platas-Iglesias, C.; Rodriguez-Blas, T. *J. Am. Chem. Soc.* **2009**, *131*, 3331–3341. (b) Gonzalez-Lorenzo, M.; Platas-Iglesias, C.; Avecilla, F.; Faulkner, S.; Pope, S. J. A.; de Blas, A.; Rodriguez-Blas, T. *Inorg. Chem.* **2005**, *44*, 4254–4262. (c) Mato-Iglesias, M.; Roca-Sabio, A.; Palinkas, Z.; Esteban-Gomez, D.; Platas-Iglesias, C.; Toth, E.; de Blas, A.; Rodriguez-Blas, T. *Inorg. Chem.* **2008**, *47*, 7840–7851.
(42) Dolg, M.; Stoll, H.; Savin, A.; Preuss, H. *Theor. Chim. Acta* **1989**, *75*, 173–194.
(43) (a) Aime, S.; Botta, M.; Fasano, M.; Marques, M. P. M.; Geraldes, C. F. G. C.; Pubanz, D.; Merbach, A. E. *Inorg. Chem.* **1997**, *36*, 2059–2068. (b) Hoeft, S.; Roth, K. *Chem. Ber.* **1993**, *126*, 869–873. (c) Aime, S.; Botta, M.; Ermondi, G. *Inorg. Chem.* **1992**, *31*, 4291–4299.
(44) Parker, D.; Dickins, R. S.; Puschmann, H.; Crossland, C.; Howard, J. A. K. *Chem. Rev.* **2002**, *102*, 1977–2010.
(45) Polasek, M.; Kotek, J.; Hermann, P.; Cisarova, I.; Binnemans, K.; Lukes, I. *Inorg. Chem.* **2009**, *48*, 466–475.

form, the aromatic ring is bent backward. Our calculations indicate that the syn conformation is the most stable one for both the SAP and TSAP forms. Furthermore, they provide relative free energies of the SAP isomer with respect to the TSAP one of −26.6 ($[Gd(L^1OH)]^-$), −1.63 ($[Gd(L^2)(H_2O)]$), and −6.92 kJ·mol^{-1} ($[Gd(L^2)(H_2O)_2]$), which suggests that the complexes adopt in solution a SAP geometry. The ^{1}H NMR spectrum of the europium complex of L^1 recorded in a D_2O solution supports this hypothesis. In DOTA-like complexes, the signals due to axial protons in the macrocyclic backbone are usually found between 24 and 36 ppm in the SAP isomer and between 5 and 12 ppm in the TSAP isomer.[46] In the case of $[Eu(L^1OH)]^-$, these signals are observed between 28 and 35 ppm (Figure S5 in the Supporting Information), which suggests that the major species in solution corresponds to the SAP form. The ^{1}H NMR spectrum of the L^2 analogue shows very broad signals, as is usually observed for N-alkylated lanthanide(III) complexes of DO3A. As a result, the positions of the signals due to axial protons of the macrocycle could not be established.

The minimum-energy conformations obtained for the $[Gd(L^1OH)]^-$ and $[Gd(L^2)(H_2O)_2]$ complexes are shown in Figure 3. For $[Gd(L^2)(H_2O)]$, the mean distance between the metal ion and the donor atoms of the carboxylate groups is 2.30 Å in both isomers, while the average Gd−N distances amount to 2.73 Å (SAP) and 2.74 Å (TSAP). The distance between the metal ion and the oxygen atom of the coordinated water molecule is slightly longer for the TSAP isomer (2.52 Å) than for the SAP one (2.50 Å), in line with a higher steric compression around the inner-sphere water molecule in the TSAP form.[47] As expected because of the increase in the coordination number, for $[Gd(L^2)(H_2O)_2]$, the bond distances of the metal coordination environment are slightly longer than those for the analogue with $q = 1$: the mean distance between the metal ion and the donor atoms of the carboxylate groups is 2.34 Å in both isomers, while the average Gd−N distances amount to 2.75 Å (SAP) and 2.78 Å (TSAP). For $[Gd(L^1OH)]^-$, the average Gd−N distances are 2.76 Å (SAP) and 2.78 Å (TSAP), while the average Gd−O distance amounts to 2.33 Å for both isomers. The calculated Gd−O bond distances are very close to those observed in the solid state for gadolinium(III) complexes with DO3A and DOTA derivatives, while the calculated Gd−N distances are typically 0.05−0.10 Å longer than those observed in the solid state.[48]

Study of the Interaction of $[Gd(L^2)]$ with Carbohydrates and α-Hydroxy Acids. The interaction of $[Gd(L^1)]$ and $[Gd(L^2)]$ with several carbohydrates such as D-(+)-glucose, D-fructose, D-galactose, and D-mannose has been followed by means of spectrophotometric titrations on 10^{-3} M solutions of the complexes (pH 7.4, MOPS buffer). Furthermore, we have also investigated the interaction of these complexes with lactate and citrate, which exist in relatively high concentration in blood and are known to bind PBAs.[49] For comparative purposes, we have also carried out spectrophotometric titrations to investigate the interaction of these saccharides and α-hydroxy acids with PBA under the same experimental conditions. In the case of $[Gd(L^1)]$, saccharide addition did not provoke any change on the absorption spectrum of the complex. Thus, we conclude that the coordination of the PBA function to the Gd^{III} ion at physiological pH prevents saccharide binding to this complex. However, the situation is very different for the L^2 analogue.

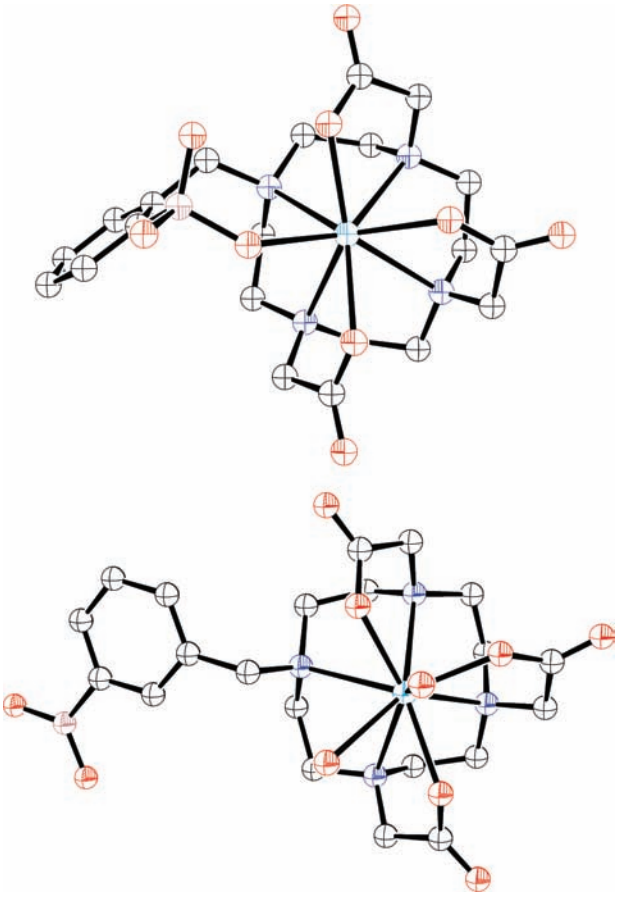

Figure 3. Minimum-energy conformations obtained from DFT calculations for the $[Gd(L^1OH)]^-$ (top) and $[Gd(L^2)(H_2O)_2]$ (bottom) systems [$\Delta(\lambda\lambda\lambda\lambda)$ forms]. Hydrogen atoms are omitted for simplicity.

The absorption spectrum of $[Gd(L^2)]$ recorded at pH 7.4 presents a weak absorption with a maximum at ca. 270 nm typical of the PBA chromophore.[31] The intensity of this band progressively decreases upon saccharide addition (Figure 4; see also Figures S6 and S7 in the Supporting Information). The addition of lactate or citrate results in similar spectral changes (Figures S8 and S9 in the Supporting Information). Nonlinear least-squares fits of the UV−vis titration profiles allowed us to determine the

(46) (a) Main, M.; Snaith, J. S.; Meloni, M. M.; Jauregui, M.; Sykes, D.; Faulkner, S.; Kenwright, A. M. *Chem. Commun.* **2008**, 5212–5214. (b) Adair, C.; Woods, M.; Zhao, P.; Pasha, A.; Winter, P. M.; Lanza, G. M.; Athey, P.; Sherry, A. D.; Kiefer, G. E. *Contrast Media Mol. Imaging* **2007**, *2*, 55–58.

(47) Woods, M.; Kovacs, Z.; Zhang, S.; Sherry, A. D. *Angew. Chem., Int. Ed.* **2003**, *42*, 5889–5892.

(48) (a) Aime, S.; Batsanov, A. S.; Botta, M.; Howard, J. A. K.; Lowe, M. P.; Parker, D. *New J. Chem.* **1999**, *23*, 669–670. (b) Chang, C. A.; Francesconi, L. C.; Malley, M. F.; Kumar, K.; Gougoutas, J. Z.; Tweedle, M. F.; Lee, D. W.; Wilson., L. J. *Inorg. Chem.* **1993**, *32*, 3501–3508. (c) Aime, S.; Anelli, P. L.; Botta, M.; Fedeli, F.; Grandi, M.; Paoli, P.; Uggeri, F. *Inorg. Chem.* **1992**, *31*, 2422–2428. (d) Platzek, J.; Blaszkiewicz, P.; Gries, H.; Luger, P.; Michl, G.; Muller-Fahrnow, A.; Raduchel, B.; Sulzle, D. *Inorg. Chem.* **1997**, *36*, 6086–6093. (e) Kumar, K.; Chang, C. A.; Francesconi, L. C.; Dischino, D. D.; Malley, M. F.; Gougoutas, J. Z.; Tweedle, M. F. *Inorg. Chem.* **1994**, *33*, 3567–3575.

(49) (a) Friedman, S.; Pace, B.; Pizer, R. *J. Am. Chem. Soc.* **1974**, *96*, 5381–5384. (b) Sartain, F. K.; Yang, X.; Lowe, C. R. *Chem.—Eur. J.* **2008**, *14*, 4060–4067.

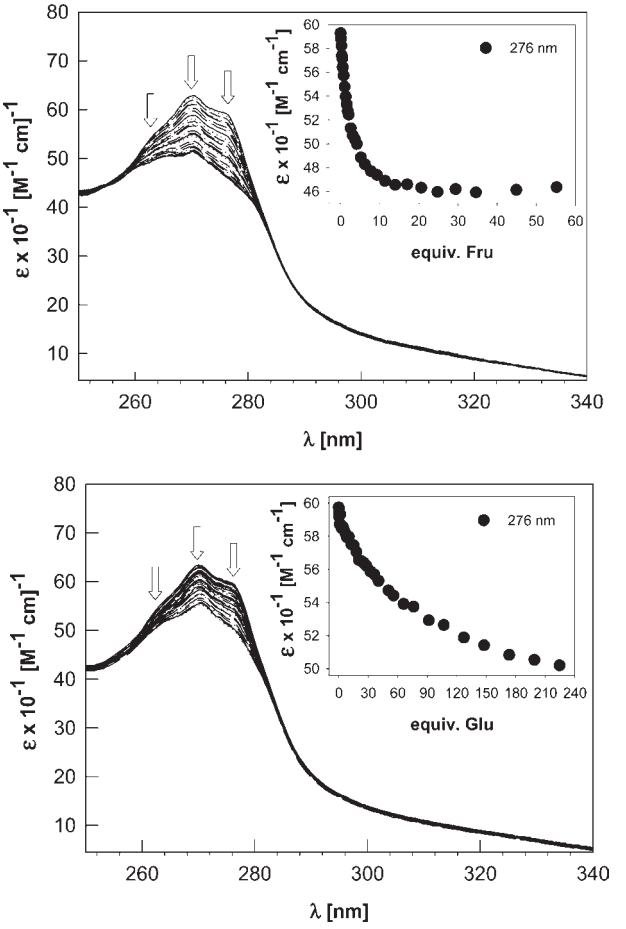

Figure 4. Spectrophotometric titrations of 10^{-3} M solutions of [Gd(L^2)] with a standard solution of D-fructose (top) or D-glucose (bottom) in an aqueous solution at pH 7.4 (0.1 M MOPS buffer). Insets: changes in the molar absorbance at 276 nm upon saccharide addition.

Table 2. Binding Constants (K_{eq} Values, M^{-1}) Determined for the Interaction of [Gd(L^2)] and PBA with Different Saccharides and α-Hydroxy Acids in an Aqueous Solution at 25 °C and pH 7.4 (0.1 M MOPS Buffer)[a]

	[Gd(L^2)]	PBA[b]	PBA[c]
D-fructose	646 ± 14	158 ± 4	160
D-(+)-glucose	12.3 ± 0.6	5.3 ± 0.1	4.6
D-galactose	24.5 ± 0.6	15.8 ± 0.4	15
D-mannose	21.9 ± 0.5	11.2 ± 0.3	13
5-acetylneuraminic acid	151 ± 4	19.1 ± 0.4	21
2-α-*O*-methyl-5-acetylneuraminic acid	79 ± 2	*d*	*d*
methyl α-D-galactoside	1.48 ± 0.03	*d*	*d*
methyl α-D-mannoside	1.38 ± 0.03	*d*	*d*
lactate	14.8 ± 0.3	25.7 ± 1.1	*d*
citrate	24.0 ± 0.5	35.5 ± 0.8	*d*

[a] The errors given correspond to 1 standard deviation. [b] This work. [c] Reference 50, 0.1 phosphate buffer. [d] Not determined.

binding constants listed in Table 2. Our results indicate the following binding affinity trend of these saccharides to [Gd(L^2)]: fructose > galactose ∼ mannose > glucose. The binding constants obtained for the interaction with PBA itself under the same conditions follow the same trend. Furthermore, the binding constants obtained for PBA by using spectrophotometric titrations (Figures S10−S15 in the Supporting Information) are very similar to those determined previously in a 0.1 M phosphate buffer using the fluorescent reporter Alizarin Red S (Table 2).[50] These results indicate that (i) the spectral changes observed in the absorption spectrum can be used to investigate the interaction of PBAs with saccharides and (ii) the nature of the buffer does not have an important effect on the binding constants. The K_{eq} values obtained for [Gd(L^2)] are somewhat higher than those obtained for PBA, with a ca. 2-fold increase being observed for glucose, galactose, and mannose. In the case of fructose, a 4-fold increase of the association constant is observed. The energy difference between the two binding processes (3.5 kJ·mol^{-1}) suggests that this could be due to differences in hydration of the host to which fructose is binding or to a favorable difference in hydration of the adduct in the case of the lanthanide(III) complex. The binding constants obtained for the interaction of [Gd(L^2)] with lactate and citrate are slightly lower than those obtained for PBA. The affinities of [Gd(L^2)] for lactate and citrate are similar to those observed for glucose and galactose, respectively.

Study of the Interaction of [Gd(L^2)] with Neu5Ac and MeNeu5Ac. The addition of Neu5Ac to solutions of PBA or [Gd(L^2)] resulted in poor changes in the absorption spectra. Furthermore, analysis of the titration curves is complicated by the absorption of saccharide in the UV region of the spectrum. Thus, we have performed competitive spectrophotometric titrations to investigate the interaction of Neu5Ac with these systems. In a typical experiment, a 10^{-3} M solution of the PBA derivative containing a given amount of Neu5Ac was prepared, and aliquots of a standard solution containing D-fructose and Neu5Ac were added. The concentration of Neu5Ac in the latter solution was identical with that used in the titration cell to keep its concentration constant during the experiment. The changes in the absorption spectrum as a function of the equivalents of D-fructose added (Figure 5; see also Figure S16 in the Supporting Information) were used to determine the binding constants for the interaction of PBA and [Gd(L^2)] with Neu5Ac because the binding constants for the interaction with D-fructose are known (Table 2). The binding constant obtained for the interaction of PBA with Neu5Ac (K_{eq} = 19) is in good agreement with that obtained in a 0.1 M phosphate buffer using the fluorescent reporter Alizarin Red S (K_{eq} = 21).[50] This result gave us confidence that the competitive assay provides accurate binding constants for the interaction of PBAs with Neu5Ac. A comparison of the titration profiles obtained upon fructose addition in the absence (Figure 4) and in the presence (Figure 5) of Neu5Ac clearly shows that in the latter case a larger excess of fructose is required to reach the plateau in which the gadolinium(III) complex is fully bound to fructose. This indicates that Neu5Ac is efficiently competing with fructose for binding to the gadolinium(III) complex. The binding constant obtained for the interaction of [Gd(L^2)] with Neu5Ac (K_{eq} = 151) is much higher than that obtained for PBA by using the same method.

Neu5Ac is present in solution as an equilibrium between α-pyranose (5−8%) and β-pyranose forms (92−95%), while the furanose type of Neu5Ac is absent because of the acetamide moiety present at the C5 position.[8] Thus, in solution, the major form of free Neu5Ac is

(50) Springsteen, G.; Wang, B. *Tetrahedron* **2002**, *58*, 5291–5300.

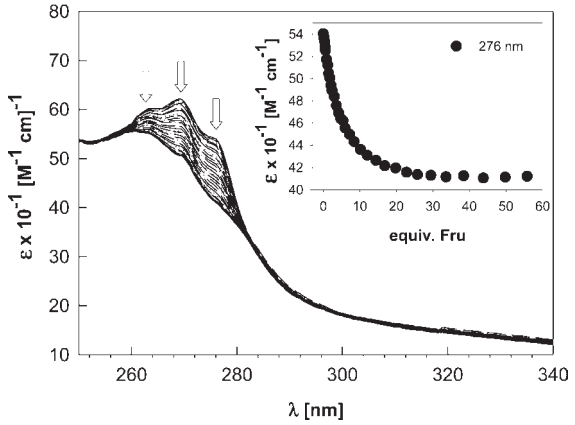

Figure 5. Spectrophotometric titration of a 10^{-3} M solution of [Gd(L^2)] containing Neu5Ac (0.01 M) with a standard solution of D-fructose in an aqueous solution at pH 7.4 (0.1 M MOPS buffer).

expected to be the β-pyranose form, while all known glycosides of Neu5Ac are α-linked.[9] Therefore, we have investigated the interaction of [Gd(L^2)] with MeNeu5Ac as a model for neuraminic residues present in the terminal positions of the carbohydrate chains (Figure S17 in the Supporting Information). A competitive assay analogous to that employed for Neu5Ac provided a binding constant for the interaction of [Gd(L^2)] with MeNeu5Ac ($K_{eq} = 79$) somewhat lower than that determined for Neu5Ac but still substantially larger than that obtained for the interaction of PBA with Neu5Ac. These results suggest that the sialic acids bind more strongly to [Gd(L^2)] when they adopt the β-pyranose form. The interaction of [Gd(L^2)] with methyl α-D-galactoside and methyl α-D-mannoside, which are models of units commonly present in glycan chains, was also investigated by means of spectrophotometric titrations (Figures S18 and S19 in the Supporting Information). Our results show that [Gd(L^2)] presents a good selectivity for both Neu5Ac and MeNeu5Ac over these saccharides (Table 2).

It has been shown that the optimal pH for the binding of boronic acids to diols is often above the pK_a value of the boronic acid species because the binding of *cis*-diols is normally stronger when PBA is in the tetrahedral form.[32] However, both PBA and [Gd(L^2)] possess very similar pK_a values, and therefore the high binding constant observed for the interaction of [Gd(L^2)] with Neu5Ac and MeNeu5Ac in comparison to PBA cannot be explained in terms of the respective pK_a values of the PBAs (8.8 and 8.9, respectively). It has been shown that ester formation with sugars lowers the pK_a value of the boron functionality by about 2−3 pH units and converts the boron atom from a neutral sp^2 to an anionic sp^3 moiety.[50] Indeed, a UV−vis pH titration of a 10^{-3} M solution of [Gd(L^2)] containing 0.05 M Neu5Ac allowed us to determine an apparent pK_a of 7.2 (Figure S20 in the Supporting Information). From these data, together with the binding constant obtained for the interaction of [Gd(L^2)] and Neu5Ac, we estimate a pK_a for the ester form of ∼7.0. Thus, upon binding to Neu5Ac at pH 7.4, the boron atom of [Gd(L^2)] is expected to be largely in the tetrahedral form. ^{11}B NMR spectroscopy confirms the change of boron hybridization upon Neu5Ac binding from trigonal ($\delta \sim$ 10 ppm) to tetrahedral ($\delta \sim -15$ ppm) form (see Figure 6).[16]

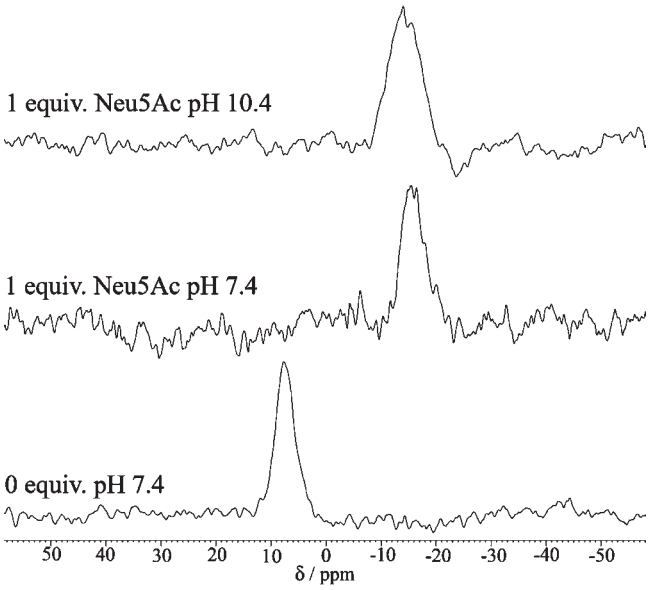

Figure 6. ^{11}B NMR spectra of a 10 mM D_2O solution of [La(L^2)] recorded in the absence and presence of 1 equiv of Neu5Ac.

The emission lifetime of the Tb($^5D_4$) excited-state level of a solution containing 10^{-3} M [Tb(L^2)] and 0.05 M Neu5Ac determined at pH 7.4 (0.1 M MOPS) amounts to 1.42 ms. This lifetime is substantially longer than that determined in the absence of Neu5Ac (1.18 ms), in agreement with the displacement of inner-sphere water molecules due to the binding of the COO^- group of Neu5Ac to the lanthanide ion. It must be pointed out that according to the binding constant reported in Table 2 under the experimental conditions used for lifetime measurements ca. 88% of the terbium(III) complex is expected to be bound to Neu5Ac. Relaxivity measurements provide additional evidence for the binding of Neu5Ac through the carboxylate group. Indeed, the addition of 10 equiv of Neu5Ac to a 1.62 mM solution of [Gd(L^2)] at 25 °C results in a decrease of relaxivity over the entire range of proton Larmor frequencies (Figure 2). In the high-field region, where relaxivity is essentially controlled by the factor $q\tau_R/r_H^6$, relaxivity decreases from ca. 7.0 $mM^{-1}\cdot s^{-1}$ to ca. 6.5 $mM^{-1}\cdot s^{-1}$ (20 MHz, 25 °C). Although this relaxivity decrease is relatively limited, even if one considers that under the experimental conditions used only 60% of the gadolinium(III) complex is expected to be bound to Neu5Ac, it clearly evidences the binding of Neu5Ac. A similar effect is observed at 37 °C (Figure S4 in the Supporting Information).

The binding of Neu5Ac to [La(L^2)] was investigated by ^{13}C NMR spectroscopy. The spectrum obtained for a solution containing 6 mM Neu5Ac and 18 mM [La(L^2)] at pD 8.6 is compared to that of free Neu5Ac in Figure 7. Under these conditions, most of Neu5Ac is bound to the lanthanum(III) complex (> 95%) because only very small peaks due to free Neu5Ac are observed. PBA is known to bind covalently and reversibly to 1,2- and 1,3-diols to give five- and six-membered cyclic esters.[21] The spectrum shown in Figure 7 is consistent with the presence of a single bound species, pointing to a very specific interaction of Neu5Ac with the lanthanum(III) complex. The resonances due to carbon nuclei of the [La(L^2)] complex

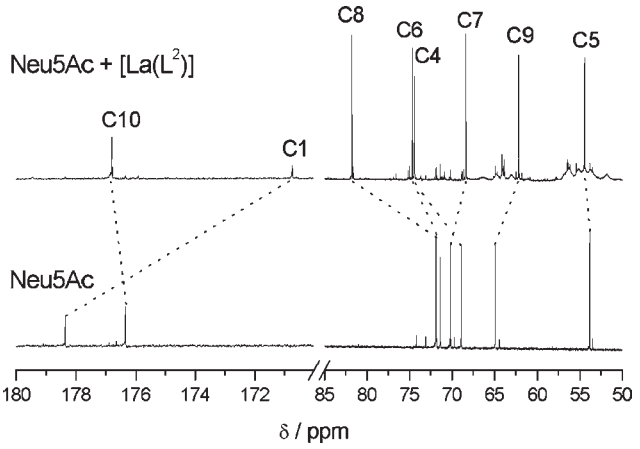

Figure 7. ^{13}C NMR spectra of Neu5Ac (6 mM) and Neu5Ac (6 mM) + [La(L^2)] (18 mM) in a D_2O solution (pD = 8.6, 25 °C). The broad resonances observed in the range of 50−70 ppm are due to carbon nuclei of the [La(L^2)] complex.

Table 3. ^1H and ^{13}C NMR Chemical Shifts (ppm) for Neu5Ac and Its Complexed Form with [La(L^2)] in D_2O at pD 8.6[a]

	free	complex		free	complex
C1	178.3	170.8	H3eq	2.16	2.94
C2	98.0	*b*	H3ax	1.76	2.79
C3	41.0	42.1	H4	3.97	4.16
C4	68.9	74.4	H5	3.85	4.31
C5	53.9	54.4	H6	3.92	3.83
C6	71.8	74.7	H7	3.46	3.47
C7	71.4	68.4	H8	3.70	3.34
C8	71.9	81.8	H9	3.56	3.72
C9	64.9	62.1	H9′	3.79	3.79
C10	176.3	176.8	H11	2.00	2.04
C11	23.7	23.5			

[a] See Chart 1 for the labeling scheme. [b] Not observed.

are extremely broad. Broad NMR signals are often observed for N-alkylated Ln^{III}(DO3A) complexes because of exchange phenomena.[51] However, the ^{13}C NMR signals due to the bound form of Neu5Ac could be assigned with the aid of 2D COSY, HSQC, and HMBC experiments. The chemical shifts observed for the bound form of Neu5Ac are compared to those of free Neu5Ac in Table 3. The assignments of the NMR signals of free Neu5Ac are in agreement with those reported in the literature.[52] The interaction with [La(L^2)] causes very important shifts of the ^{13}C NMR signals of Neu5Ac. In particular, the signal due to the carboxylate group of Neu5Ac (C1) shifts upfield by 7.6 ppm, while the signal due to C10 is little affected. These results are consistent with the binding of the carboxylate function of Neu5Ac to the lanthanide. The carbon nuclei of the glycerol tail of Neu5Ac also experience important shifts upon binding to [La(L^2)]. In particular, a downfield shift of 9.9 ppm is observed for C8, while C7 and C9 undergo upfield shifts of 1.8 and 2.7 ppm, respectively. It has been previously shown that the formation of a five-membered ester at C7 and C8 is limited by the unfavorable erythro configuration of the glycerol tail,[53] while the formations of a five-membered cyclic ester at C8 and C9 and a six-membered cyclic ester at C7 and C9 are both possible. The very large shift observed for C8 suggests that the binding to the glycerol tail occurs through C8 and C9. The ^1H NMR spectral data further support a binding at positions 8 and 9 because the signal due to H8 experiences an important upfield shift upon binding (0.45 ppm), while the chemical shift of H7 remains nearly unaffected. The H3−H5 ^1H NMR signals of Neu5Ac also undergo important downfield shifts upon binding to [La(L^2)] (0.19−0.78 ppm). Thus, the lanthanide(III) complexes of L^2 appear to bind to Neu5Ac through a cooperative two-site binding through (i) ester formation by the interaction on the PBA function of the receptor and (ii) coordination of the carboxylate function of Neu5Ac to the Ln^{III} ion.

In order to rationalize the selectivity that [Gd(L^2)] shows for Neu5Ac, we have characterized the [Gd(L^2OH)·Neu5Ac]$^{2-}$ system by means of DFT calculations in the gas phase (B3LYP model). Different computational studies have shown that this computational approach provides molecular geometries in good agreement with the solution structures of the complexes.[41] The main difference between the gas-phase geometries and the actual solution structures is the Ln−N distances, which are overestimated with calculations performed in the gas phase by ca. 0.1 Å.[54] For the reasons given above, our calculations were performed for both the α-pyranose and β-pyranose forms of Neu5Ac. PBA is known to bind covalently and reversibly to 1,2- and 1,3-diols to give five- and six-membered cyclic esters.[16] It has been previously shown that the formation of a five-membered ester at C7 and C8 is limited by the unfavorable erythro configuration of the glycerol tail.[53] Thus, we have only considered in our calculations the five-membered cyclic ester formed at C8 and C9 and the six-membered cyclic ester formed at C7 and C9 (Chart 1). Geometry optimizations provided up to eight energy minima that correspond to combinations of the SAP and TSAP conformations of the Gd^{III}-(DO3A) cage forming esters with the α-pyranose and β-pyranose forms of Neu5Ac at the C8−C9 and C7−C9 positions. The relative free energies of the different conformations obtained as a result of geometry optimizations are given in Table 4. Our results show that the adduct formed at C8 and C9 is more stable than that formed at C7 and C9 for both the α-pyranose and β-pyranose forms of Neu5Ac, in nice agreement with the NMR data. The adducts formed by the SAP form of the complex are more stable than those formed by the TSAP one. Furthermore, our results suggest that the binding to the β-pyranose form of Neu5Ac is slightly more favorable than that to the α-pyranose conformation. The two lowest-energy conformations calculated for the [Gd(L^2OH)·Neu5Ac]$^{2-}$ system are shown in Figure 8. The carboxylate unit of Neu5Ac is predicted to bind to the Gd^{III} ion in a slightly asymmetrical bidentate fashion, with the $Gd^{III}-O_{Neu5Ac}$

(51) Lowe, M. P.; Parker, D.; Reany, O.; Aime, S.; Botta, M.; Castellano, G.; Gianolio, E.; Pagliarin, R. *J. Am. Chem. Soc.* **2001**, *123*, 7601–7609.
(52) (a) Czarniecki, M. F.; Thornton, E. R. *J. Am. Chem. Soc.* **1977**, *99*, 8273–8279. (b) Gervay, J.; Batta, G. *Tetrahedron Lett.* **1994**, *35*, 3009–3012. (c) Klepach, T.; Zhang, W.; Carmichael, I.; Serianni, A. S. *J. Org. Chem.* **2008**, *73*, 4376–4387.
(53) Chai, W.; Yuen, C.-T.; Feizi, T.; Lawson, A. M. *Anal. Biochem.* **1999**, *270*, 314–322.
(54) (a) Cosentino, U.; Villa, A.; Pitea, D.; Moro, G.; Barone, V.; Maiocchi, A. *J. Am. Chem. Soc.* **2002**, *124*, 4901–4909. (b) Platas-Iglesias, C.; Mato-Iglesias, M.; Djanashvili, K.; Muller, R. N.; Vander Elst, L.; Peters, J. A.; de Blas, A.; Rodriguez-Blas, T. *Chem.—Eur. J.* **2004**, *10*, 3579–3590.

Table 4. Relative Free Energies ($kJ \cdot mol^{-1}$) of the Different Conformations Obtained for the $[Gd(L^2OH) \cdot Neu5Ac]^{2-}$ System by Means of DFT Calculations (B3LYP Model) Compared to the Complex with the Lowest Energy[a]

	α-Neu5Ac	β-Neu5Ac
SAP(C8−C9)	5.8	0.0
SAP(C7−C9)	77.9	42.0
TSAP(C8−C9)	9.7	7.9
TSAP(C7−C9)	70.7	33.7

[a] SAP and TSAP indicate square-antiprismatic and twisted square-antiprismatic geometries, respectively; relative energies of esters formed at both the C8−C9 and C7−C9 positions are given.

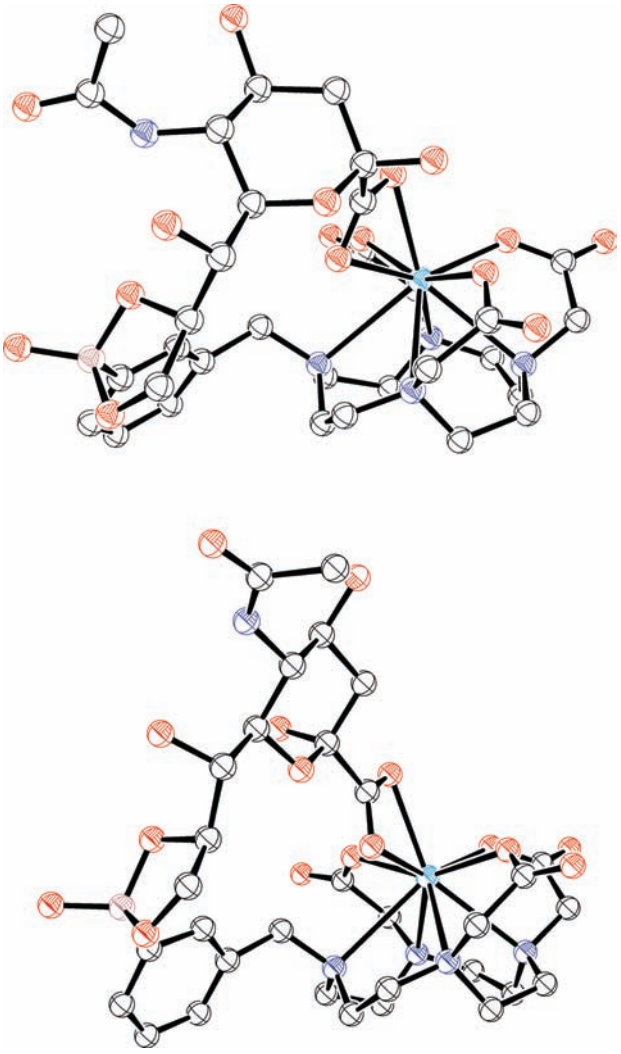

Figure 8. Optimized structures of the $[Gd(L^2OH) \cdot Neu5Ac]^{2-}$ system obtained from DFT calculations at the B3LYP/6-31G(d) level. Top: α-pyranose form of Neu5Ac. Bottom: β-pyranose form of Neu5Ac. Hydrogen atoms are omitted for simplicity.

distances amounting to 2.49 and 2.53 Å (α-pyranose) and 2.53 and 2.56 Å (β-pyranose). Thus, our DFT calculations confirm that a two-site cooperative binding of Neu5Ac to $[Gd(L^2)]$ is possible for both the α- and β-pyranose conformations.

Conclusions

In conclusion, we have described a straightforward approach to preparing the first example of a new family of lanthanide complexes for sialic acid recognition due to a cooperative two-site binding through (i) ester formation by the interaction on the PBA function of the receptor and (2) coordination of the carboxylate function of Neu5Ac to the Ln^{III} ion. Compared with simple PBA, complex $[Gd(L^2)]$ represents an improvement of about 8-fold in affinity and about 3.4-fold in selectivity for Neu5Ac over glucose, the most common saccharide present in vivo. Furthermore, $[Gd(L^2)]$ also shows a good selectivity for Neu5Ac over lactate and citrate, which occur in relatively high concentration in blood. On the contrary, PBA forms stronger complexes with both lactate and citrate than with Neu5Ac.

The binding affinity for MeNeu5Ac, a model for sialic acid residues on cell surfaces, is somewhat lower than that for free Neu5Ac. However, a much weaker binding affinity was observed with methyl α-D-galactoside and methyl α-D-mannoside, which are models of units commonly present in glycan chains. Thus, this receptor shows promise for the preparation of new sensors for sialic acid recognition on cell surfaces and radiopharmaceuticals for the diagnosis and therapy of tumors. Furthermore, we believe that the general approach reported here can be used to design more effective receptors. For instance, lowering the pK_a of the PBA function should increase the binding affinity of the receptor to the glycerol tail of sialic acids, while increasing the positive charge of the lanthanide chelate will strengthen the binding to the carboxylate group of Neu5Ac. By contrast to the complexes of L^2, the L^1 analogues do not bind to sugars because of an unprecedented coordination of the phenylboronate function of the ligand to the Ln^{III} ion.

Experimental Section

Physical Methods. Elemental analyses were carried out on a ThermoQuest Flash 1112 elemental analyzer. Electrospray ionization time-of-flight (ESI-TOF) mass spectra were recorded using a LC-Q-q-TOF Applied Biosystems QSTAR Elite spectrometer in both positive and negative modes. Fast atom bombardment (FAB) mass spectra were recorded using a FISONS QUATRO mass spectrometer with a Cs-ion gun and 3-nitrobenzyl alcohol as the matrix. IR spectra were recorded using a Bruker Vector 22 spectrophotometer equipped with a Golden Gate attenuated total reflectance (ATR) accessory (Specac). ^1H and ^{13}C NMR spectra were run on a Bruker Avance 500 spectrometer. Chemical shifts are reported in δ values. ^{11}B NMR spectra was measured on a Bruker Avance 400 spectrometer using a solid-state probe and 4 mm zirconia rotors, spinning at the magic angle with a rate of 20 Hz. Peak positions were measured with respect to the resonance of a 0.1 M solution of boric acid (0 ppm). Electronic spectra in the UV−vis range were recorded at 25 °C on a Perkin-Elmer Lambda 900 UV−vis spectrophotometer using 1.0 cm quartz cells. Sugar binding studies were performed on 10^{-3} M solutions of PBA or $[Gd(L^2)]$ (10 mL) at pH 7.4 (MOPS buffer). Typically, aliquots of a fresh standard solution of the envisaged saccharide (ca. 0.5 M; containing 10^{-3} M PBA or $[Gd(L^2)]$ to avoid dilution) were added, and the UV−vis spectra of the samples were recorded. Glucose solutions were allowed to stand at least 24 h to allow them to reach anomeric equilibrium. Competitive UV−vis titrations were performed in a similar way by using 0.05 or 0.01 M Neu5Ac in the titration cell for PBA and $[Gd(L^2)]$, respectively. An analogous competitive assay was used to investigate the binding of MeNeu5Ac to $[Gd(L^2)]$. In order to keep the Neu5Ac concentration constant during the titration aliquots of a standard solution containing D-fructose (0.5 M), Neu5Ac (0.05 or 0.01 M) and the PBA derivative (10^{-3} M) were added, and the UV−vis spectra of the samples were recorded. All spectrophotometric titration curves were fitted with the

HYPERQUAD program.[55] Binding constants were obtained from a simultaneous fit of the UV−vis absorption spectral changes at 6−8 selected wavelengths. A minimum of 25 absorbance data points at each of these wavelengths was used. Excitation and emission spectra were recorded on a Perkin-Elmer LS-50B spectrometer. Luminescence lifetimes were calculated from the monoexponential fitting of the average decay data, and they are averages of at least 3−5 independent determinations.

The $1/T_1$ NMRD profiles of the gadolinium(III) complexes were recorded on a Stelar SMARtracer FFC fast-field-cycling relaxometer covering magnetic fields from 2.35×10^{-4} to 0.25 T, which correspond to a proton Larmor frequency range of 0.01−10 MHz. The relaxivity at higher fields was recorded using a Bruker WP80 adapted to variable field measurements and controlled by the SMARtracer PC-NMR console. The temperature was controlled by a VTC90 temperature control unit and fixed by a gas flow. The temperature was determined according to previous calibration with a platinum resistance temperature probe.

Computational Methods. All calculations were performed by employing hybrid DFT with the B3LYP exchange-correlation functional,[56,57] and the *Gaussian 03* package (revision C.01).[58] Relativistic effects were considered through the use of relativistic ECPs (RECPs). Different computational studies on lanthanide(III) complexes have shown that the 4f orbitals do not participate in bonding because of their contraction into the core.[59] Thus, full geometry optimizations of the $[Gd(L^1OH)]^-$, $[Gd(L^2)(H_2O)]$, $[Gd(L^2)(H_2O)_2]$, and $[Gd(L^2OH)\cdot Neu5Ac]^{2-}$ systems were performed in vacuo by using the RECP of Dolg et al. and the related [5s4p3d]-GTO valence basis set for the gadolinium atom[42] and the 6-31G(d) basis set for carbon, hydrogen, boron, nitrogen, and oxygen atoms. The RECP of Dolg et al. includes $46 + 4f^7$ electrons in the core for the gadolinium atom, leaving the outermost 11 electrons to be treated explicitly, in line with the nonparticipation of 4f electrons in bonding. Thus, this RECP treats $[Kr]4d^{10}4f^7$ as a fixed core, while only the $5s^25p^66s^25d^16p^0$ shell is explicitly taken into account. The stationary points found on the potential energy surfaces as a result of the geometry optimizations on the $[Gd(L^1OH)]^-$, $[Gd(L^2)(H_2O)]$, $[Gd(L^2)(H_2O)_2]$, and $[Gd(L^2OH)\cdot Neu5Ac]^{2-}$ systems have been tested to represent energy minima rather than saddle points via frequency analysis. The relative free energies of the different conformations calculated for these systems include non-potential-energy contributions (that is, zero point energy and thermal terms) obtained by frequency analysis.

Chemicals and Starting Materials. (2-Methylphenyl)ethyleneboronate (**1**)[29] and 5,5-dimethyl-2-*o*-tolyl-1,3-dioxa-2-borinane (**3**)[27] were prepared according to literature procedures. All other chemicals were purchased from commercial sources and used without further purification. Solvents were of reagent grade, purified by the usual methods.

[2-(Bromomethyl)phenyl]ethyleneboronate (2). This compound was prepared by using a slight modification of the literature procedure.[29] A mixture of **1** (0.96 g, 5.93 mmol), NBS (1.11 g, 6.22 mmol), and PDB (0.090 g, 0.370 mmol) in CCl_4 (20 mL) was refluxed for 16 h. The reaction mixture was allowed to cool to room temperature, the precipitated succinimide was removed by filtration, and the filtrate was concentrated under reduced pressure. The crude product was purified by column chromatography on SiO_2 with CH_2Cl_2 as the eluent to give 0.570 g of **2** as a yellow hygroscopic solid. Yield: 40%. Elem anal. Calcd for $C_9H_{10}BBrO_2$: C, 44.87; H, 4.18. Found: C, 45.01; H, 4.25. MS (ESI$^-$): m/z 239 ($[C_9H_9BBrO_2]^-$). IR (ATR, cm^{-1}): ν 3064, 2987, 2913 (C−H), 1597 (C═C), 1325 (C−B). ^{1}H NMR ($CDCl_3$, 500 MHz, 25 °C, TMS): δ 7.86 (d, 1H, ArH), 7.45 (m, 2H, ArH), 7.31 (m, 1H, ArH), 4.92 (s, 2H, CH_2Br), 4.42 (s, 4H, OCH_2). ^{13}C NMR ($CDCl_3$, 125.8 MHz, 25 °C, TMS): δ 144.3, 136.7, 131.6, 130.3, 127.7, 66.0, 33.8.

2-[2-(Bromomethyl)phenyl]-5,5-dimethyl-1,3-dioxa-2-borinane (4). This compound was prepared by using a slight modification of the literature procedure.[27] A mixture of **3** (1.22 g, 5.98 mmol), NBS (1.12 g, 6.28 mmol), and PDB (0.090 g, 0.370 mmol) in CCl_4 (20 mL) was refluxed for 16 h. The reaction mixture was allowed to cool to room temperature, the precipitated succinimide was removed by filtration, and the filtrate was concentrated under reduced pressure. The crude product was purified by column chromatography on SiO_2 with CH_2Cl_2 as the eluent to give 1.39 g of **4** as a yellow oil. Yield: 82%. Elem anal. Calcd for $C_{12}H_{16}BBrO_2$: C, 50.93; H, 5.70. Found: C, 50.47; H, 5.57. MS (FAB): m/z(% BPI) 203(100) ($[C_{12}H_{16}BO_2]^+$), 283(10) ($[C_{12}H_{17}BBrO_2]^+$). IR (ATR, cm^{-1}): ν 2959, 2935, 2871 (C−H), 1599 (C═C), 1321 (C−B). ^{1}H NMR ($CDCl_3$, 500 MHz, 25 °C, TMS): δ 7.81 (d, 1H, ArH), 7.37 (m, 1H, ArH), 7.28 (m, 2H, ArH), 4.93 (s, 2H, CH_2Br), 3.82 (s, 4H, OCH_2), 1.07 (s, 6H, $-CH_3$). ^{13}C NMR ($CDCl_3$, 125.8 MHz, 25 °C, TMS): δ 143.5, 135.5, 130.5, 130.2, 127.5, 72.4, 34.5, 31.8, 21.9.

1,4,7-Tris[(*tert*-butoxycarbonyl)methyl]-10-[2-(2-methylphenyl)-1,3-dioxa-2-borolanyl]-1,4,7,10-tetraazacyclododecane (5). Compound **2** (0.140 g, 0.576 mmol) and Na_2CO_3 (0.250 g, 2.359 mmol) were added to a solution of DO3A(*t*-BuO)$_3$ (0.300 g, 0.583 mmol) in acetonitrile (25 mL). The mixture was heated to reflux with stirring under an inert atmosphere (Ar) for a period of 24 h, and then the excess of Na_2CO_3 was filtered off and the filtrate concentrated to dryness. The residue was partitioned between H_2O and CH_3Cl (20:10), and the organic phase was separated, dried over $MgSO_4$, filtered, and evaporated to dryness. The crude product was purified by column chromatography on Al_2O_3 with a CH_2Cl_2/MeOH 5% mixture as the eluent to give 0.310 g of **5** as a brown oil. Yield: 63%. Elem anal. Calcd for $C_{35}H_{59}BN_4O_8\cdot 2CH_2Cl_2$: C, 52.62; H, 7.52; N, 6.63. Found: C, 51.80; H, 7.73; N, 6.79. MS (ESI$^+$): m/z 649 ($[C_{33}H_{58}BN_4O_8]^+$). IR (ATR, cm^{-1}): ν 2976, 2931, 2846 (C−H), 1724 (C═O), 1597 (C═C), 1366 (C−B). ^{1}H NMR ($CDCl_3$, 500 MHz, 25 °C, TMS): δ 7.73 (d, 1H, ArH), 7.58 (d, 1H, ArH), 7.21 (m, 1H, ArH), 7.13 (m, 1H, ArH), 4.25 (s, 4H, OCH_2), 3.71−2.05 (m, 24H, $-NCH_2-$), 1.33 (s, 27H, $-O^tBu$). ^{13}C NMR ($CDCl_3$, 125.8 MHz, 25 °C, TMS): δ 172.8, 172.5, 171.9, 143.6, 135.9, 131.0, 129.2, 126.1, 116.2, 82.2, 82.0, 81.9, 77.2, 65.4, 56.9, 56.1, 55.3, 55.2, 55.1, 49.6, 27.5, 27.4.

(3-Methylphenyl)ethyleneboronate (6). A mixture of (3-methylphenyl)boronic acid (1.00 g, 7.36 mmol) and ethylene glycol (0.59 g, 9.56 mmol) in dry toluene (25 mL) was refluxed for 20 h using a Dean−Stark apparatus for water removal. The reaction mixture was concentrated at reduced pressure, and the product was purified by column chromatography on SiO_2 with CH_2Cl_2 as the eluent to give 1.01 g of **6** as a colorless oil. Yield: 85%. Elem anal. Calcd for $C_9H_{11}BO_2$: C, 66.73; H, 6.84. Found: C, 66.56; H, 6.81. MS (FAB): m/z 162 (100%) ($[C_9H_{11}BO_2]^+$). IR (ATR, cm^{-1}): ν 3024, 2975, 2908 (C−H), 1607 (C═C), 1336 (C−B). ^{1}H NMR ($CDCl_3$, 500 MHz, 25 °C, TMS): δ 7.65 (m, 2H, ArH), 7.31 (m, 2H, ArH), 4.39 (s, 4H, OCH_2), 2.39 (s, 3H, CH_3). ^{13}C NMR ($CDCl_3$, 125.8 MHz, 25 °C, TMS): δ 137.2, 135.5, 132.2, 131.8, 127.8, 66.0, 21.3.

[3-(Bromomethyl)phenyl]ethyleneboronate (7). A mixture of **6** (1.01 g, 6.23 mmol), NBS (1.17 g, 6.55 mmol), and PDB (0.095 g, 0.380 mmol) in CCl_4 (20 mL) was refluxed for 16 h. The reaction mixture was allowed to cool to room temperature, the precipitated succinimide was removed by filtration, and the filtrate was concentrated under reduced pressure. The crude product was purified by column chromatography on SiO_2 with CH_2Cl_2 as the eluent to give 0.81 g of **7** as a yellow oil. Yield: 54%. Elem anal. Calcd for $C_9H_{10}BBrO_2$: C, 44.87; H, 4.18. Found: C, 45.13; H, 4.21. MS (ESI$^+$): m/z 161 ($[C_9H_{10}BO_2]^+$). IR (ATR, cm^{-1}): ν 3025, 2976, 2908 (C−H), 1605 (C═C), 1338 (C−B). ^{1}H NMR

(55) Gans, P.; Sabatini, A.; Vacca, A. *Talanta* **1996**, *43*, 1739–1753.
(56) Becke, A. D. *J. Chem. Phys.* **1993**, *98*, 5648–5652.
(57) Lee, C.; Yang, W.; Parr, R. G. *Phys. Rev. B* **1988**, *37*, 785–789.
(58) Frisch, M. J.; et al. *Gaussian03*, revision C.01; Gaussian, Inc.: Wallingford, CT, 2004.
(59) (a) Maron, L.; Eisenstein, O. *J. Phys. Chem. A* **2000**, *104*, 7140–7143. (b) Boehme, C.; Coupez, B.; Wipff, G. *J. Phys. Chem. A* **2002**, *106*, 6487–6498.

($CDCl_3$, 500 MHz, 25 °C, TMS): δ 7.85 (s, 1H, ArH), 7.61 (d, 1H, ArH), 7.52 (d, 1H, ArH), 7.38 (m, 1H, ArH), 4.51 (s, 2H, CH_2Br), 4.39 (s, 4H, OCH_2). ^{13}C NMR ($CDCl_3$, 125.8 MHz, 25 °C, TMS): δ 136.2, 135.4, 134.9, 132.1, 128.4, 66.1, 33.4.

1,4,7-Tris[(*tert*-butoxycarbonyl)methyl]-10-[2-(3-methylphenyl)-1,3-dioxa-2-borolanyl]-1,4,7,10-tetraazacyclododecane (8). Compound **7** (0.140 g, 0.576 mmol) and Na_2CO_3 (0.250 g, 2.359 mmol) were added to a solution of DO3A(*t*-BuO)$_3$ (0.300 g, 0.583 mmol) in acetonitrile (25 mL). The mixture was heated to reflux with stirring under an inert atmosphere (Ar) for a period of 24 h, and then the excess of Na_2CO_3 was filtered off and the filtrate concentrated to dryness. The residue was partitioned between H_2O and CH_3Cl (20:10), and the organic phase was separated, dried over $MgSO_4$, filtered, and evaporated to dryness. The crude product was purified by column chromatography on Al_2O_3 with a CH_2Cl_2/MeOH 5% mixture as the eluent to give 0.330 g of **8** as a brown oil. Yield: 67%. Elem anal. Calcd for $C_{35}H_{59}BN_4O_8 \cdot 2CH_2Cl_2$: C, 52.62; H, 7.52; N, 6.63. Found: C, 52.90; H, 7.75; N, 6.78. MS (ESI$^+$): m/z 649 ($[C_{33}H_{58}BN_4O_8]^+$). IR (ATR, cm^{-1}): ν 2970, 2929, 2849 (C−H), 1720 (C=O), 1601 (C=C), 1309 (C−B). ^1H NMR ($CDCl_3$, 500 MHz, 25 °C, TMS): δ 7.52 (s, 1H, ArH), 7.30 (d, 1H, ArH), 7.13 (d, 1H, ArH), 6.90 (m, 1H, ArH), 3.32 (s, 4H, OCH_2), 2.63−1.79 (m, 24H, $-NCH_2-$), 1.08 (s, 27H, $-O^tBu$). ^{13}C NMR ($CDCl_3$, 125.8 MHz, 25 °C, TMS): δ 172.1, 171.3, 135.1, 134.7, 132.0, 131.2, 126.6, 115.6, 81.4, 81.1, 77.2, 70.9, 58.2, 54.6, 54.3, 49.2, 48.4, 30.6, 26.7, 26.6.

1,4,7-Tris(carboxymethyl)-10-[2-(dihydroxyboranyl)benzyl]-1,4,7,10-tetraazacyclododecane Trifluoroacetate Salt ($H_3L^1 \cdot 3CF_3COOH$). A solution of compound **5** (0.310 g, 0.368 mmol) in a 1:1 CH_2Cl_2/TFA mixture (5 mL) was stirred at room temperature for 24 h. The mixture was concentrated to dryness, and the resulting oil was dissolved in methanol (∼1 mL). The addition of diethyl ether resulted in the formation of a white solid, which was collected by filtration and dried under vacuum. Yield: 0.230 g, 75%. Elem anal. Calcd for $C_{21}H_{33}BN_4O_8 \cdot 3CF_3COOH$: C, 39.43; H, 4.41; N, 6.81. Found: C, 39.04; H, 4.56; N, 7.15. MS (ESI$^-$): m/z 461 ($[C_{21}H_{30}BN_4O_7]^-$). IR (ATR, cm^{-1}): ν 3085 (C−H), 1726, 1659 (C=O), 1353 (C−B). ^1H NMR (D_2O, pD = 0.6, 500 MHz, 25 °C, ^{t}BuOH): δ 7.80 (m, 1H, ArH), 7.54−7.46 (m, 3H, ArH), 4.62−2.97 (m, 24H, CH_2).

1,4,7-Tris(carboxymethyl)-10-[3-(dihydroxyboranyl)benzyl]-1,4,7,10-tetraazacyclododecane Trifluoroacetate Salt ($H_3L^2 \cdot 3CF_3COOH$). A solution of compound **8** (0.330 g, 0.391 mmol) in a 1:1 CH_2Cl_2/TFA mixture (5 mL) was stirred at room temperature for 24 h. The mixture was concentrated to dryness, and the resulting oil was dissolved in methanol (∼1 mL). The addition of diethyl ether resulted in the formation of a white solid that was collected by filtration and dried under vacuum. Yield: 0.265 g, 82%. Elem anal. Calcd for $C_{21}H_{33}BN_4O_8 \cdot 3CF_3COOH$: C, 39.43; H, 4.41; N, 6.81. Found: C, 39.13; H, 4.48; N, 7.20. MS (ESI$^-$): m/z 461 ($[C_{21}H_{30}BN_4O_7]^-$). IR (ATR, cm^{-1}): ν 3092 (C−H), 1722, 1661 (C=O), 1357 (C−B). ^1H NMR (D_2O, pD = 0.6, 500 MHz, 25 °C, ^{t}BuOH): δ 7.83 (m, 2H, ArH), 7.62 (d, 1H, ArH), 7.48 (m, 2H, ArH), 4.48−2.82 (m, 24H, CH_2).

General Procedure for Preparation of the $[Ln(L^1)] \cdot 2H_2O$ and $[Ln(L^2)] \cdot 4H_2O$ Complexes. A mixture of $H_3L^1 \cdot 3CF_3COOH$ or $H_3L^2 \cdot 3CF_3COOH$ (0.100 g, 0.122 mmol), triethylamine (0.074 g, 0.732 mmol), and Ln(OTf)$_3$ (0.122 mmol, Ln = La, Eu, Gd, or Tb) in 2-propanol (10 mL) was heated to reflux for 24 h. The reaction was allowed to cool to room temperature and then concentrated to dryness. The addition of 5 mL of THF (L^1) or acetonitrile (L^2) resulted in the formation of a white precipitate, which was isolated by filtration. The solid was then suspended in 10 mL of THF (L^1) or acetonitrile (L^2) and stirred at room temperature for 24 h. The solid was isolated by filtration, washed with acetonitrile and diethyl ether, and dried under vacuum.

$[La(L^1)] \cdot 2H_2O$. Yield: 0.063 g, 79%. Elem anal. Calcd for $C_{21}H_{34}BLaN_4O_{10}$: C, 38.67; H, 5.25; N, 8.59. Found: C, 38.29; H, 4.83; N, 8.25. MS (ESI$^+$): m/z 617 $[C_{21}H_{31}BLaN_4O_8]^+$. IR (ATR, cm^{-1}): ν 1581 (C=O), 1395 (C−B), 1254 (B−O).

$[Eu(L^1)] \cdot 2H_2O$. Yield: 0.058 g, 72%. Elem anal. Calcd for $C_{21}H_{34}BEuN_4O_{10}$: C, 37.91; H, 5.15; N, 8.42. Found: C, 37.73; H, 4.73; N, 8.25. MS (ESI$^+$): m/z 631 $[C_{21}H_{31}BEuN_4O_8]^+$. IR (ATR, cm^{-1}): ν 1587 (C=O), 1378 (C−B), 1253 (B−O).

$[Gd(L^1)] \cdot 2H_2O$. Yield: 0.049 g, 60%. Elem anal. Calcd for $C_{21}H_{34}BGdN_4O_{10}$: C, 37.61; H, 5.11; N, 8.36. Found: C, 37.22; H, 4.82; N, 8.50. MS (ESI$^+$): m/z 636 $[C_{21}H_{31}BGdN_4O_8]^+$. IR (ATR, cm^{-1}): ν 1576 (C=O), 1385 (C−B), 1247 (B−O).

$[Tb(L^1)] \cdot 2H_2O$. Yield: 0.053 g, 65%. Elem anal. Calcd for $C_{21}H_{34}BN_4O_{10}Tb$: C, 37.52; H, 5.10; N, 8.33. Found: C, 37.03; H, 4.77; N, 8.27. MS (ESI$^+$): m/z 637 $[C_{21}H_{31}BN_4O_8Tb]^+$. IR (ATR, cm^{-1}): ν 1583 (C=O), 1377 (C−B), 1246 (B−O).

$[La(L^2)] \cdot 4H_2O$. Yield: 0.045 g, 54%. Elem anal. Calcd for $C_{21}H_{38}BLaN_4O_{12}$: C, 36.65; H, 5.56; N, 8.14. Found: C, 36.43; H, 5.46; N, 8.12. MS (ESI$^+$): m/z 617 $[C_{21}H_{31}BLaN_4O_8]^+$, 639 $[C_{21}H_{30}BLaN_4NaO_8]^+$. IR (ATR, cm^{-1}): ν 1575 (C=O), 1381 (C−B), 1252 (B−O).

$[Eu(L^2)] \cdot 4H_2O$. Yield: 0.049 g, 57%. Elem anal. Calcd for $C_{21}H_{38}BEuN_4O_{12}$: C, 35.96; H, 5.46; N, 7.99. Found: C, 35.88; H, 4.94; N, 8.22. MS (ESI$^+$): m/z 631 $[C_{21}H_{31}BEuN_4O_8]^+$. IR (ATR, cm^{-1}): ν 1586 (C=O), 1376 (C−B), 1245 (B−O).

$[Gd(L^2)] \cdot 4H_2O$. Yield: 0.054 g, 64%. Elem anal. Calcd for $C_{21}H_{38}BGdN_4O_{12}$: C, 35.70; H, 5.42; N, 7.93. Found: C, 35.32; H, 5.19; N, 7.68. MS (ESI$^+$): m/z 636 $[C_{21}H_{31}BGdN_4O_8]^+$. IR (ATR, cm^{-1}): ν 1587 (C=O), 1378 (C−B), 1248 (B−O).

$[Tb(L^2)] \cdot 4H_2O$. Yield: 0.047 g, 55%. Elem anal. Calcd for $C_{21}H_{38}BN_4O_{12}Tb$: C, 35.61; H, 5.41; N, 7.91. Found: C, 35.13; H, 4.97; N, 7.81. MS (ESI$^+$): m/z 637 $[C_{21}H_{31}BN_4O_8Tb]^+$, 659 $[C_{21}H_{30}BN_4NaO_8Tb]^+$. IR (ATR, cm^{-1}): ν 1589 (C=O), 1378 (C−B), 1247 (B−O).

Acknowledgment. The authors thank Ministerio de Educación y Ciencia and FEDER (Grant CTQ2006-07875/PPQ) and Xunta de Galicia (Grant INCITE08ENA103005ES) for financial support. This research was performed in the framework of the EU COST Action D38 "Metal-Based Systems for Molecular Imaging Applications". The authors are indebted to Centro de Supercomputación de Galicia (CESGA) for providing the computer facilities. M.R.-F. thanks Ministerio de Educación y Ciencia (FPU program) for a predoctoral fellowship. The authors gratefully acknowledge Dr. Joop A. Peters for fruitful scientific discussions.

Supporting Information Available: UV−vis spectra of PBA as a function of the pH, ^{11}B NMR spectra of $[La(L^2)]$ as a function of the pH, excitation and emission spectra of $[Tb(L^1)]$ and $[Tb(L^2)]$, spectrophotometric titrations of $[Gd(L^2)]$ with D-galactose and D-mannose, spectrophotometric titrations of PBA with different saccharides, spectrophotometric titrations of $[Gd(L^2)]$ and Me-Neu5Ac with D-fructose, spectrophotometric titrations of $[Gd(L^2)]$ with methyl α-D-galactoside and methyl α-D-mannoside, UV−vis pH titrations of $[Gd(L^2)]$ in the presence of Neu5Ac, Cartesian coordinates of the $[Gd(L^1OH)]^-$, $[Gd(L^2)(H_2O)]$, $[Gd(L^2)(H_2O)_2]$, and $[Gd(L^2OH) \cdot Neu5Ac]^{2-}$ systems optimized in vacuo (B3LYP), and complete ref 51. This material is available free of charge via the Internet at http://pubs.acs.org.